ELSEVIER

Ceramics International 29 (2003) 19–25

CERAMICS INTERNATIONAL

www.elsevier.com/locate/ceramint

Properties and microstructure of machinable $Al_2O_3/LaPO_4$ ceramic composites

Ruigang Wang*, Wei Pan, Jian Chen, Mengning Jiang, Yongming Luo, Minghao Fang

State Key Lab of New Ceramics and Fine Processing, Department of Materials Science and Engineering, Tsinghua University, Beijing 100084, People's Republic of China

Received 6 September 2001; received in revised form 5 February 2002; accepted 4 March 2002

Abstract

Layer structured $LaPO_4$ was added to Al_2O_3 ceramic matrix to improve the machinability of the composites. Densification, hardness and microstructures of the $Al_2O_3/LaPO_4$ ceramic composites have been studied at various sintering temperatures (1300, 1400, 1500, 1600 °C) and different $LaPO_4$ contents (pure Al_2O_3, 10 wt.% $LaPO_4$, 20 wt.% $LaPO_4$, 30 wt.% $LaPO_4$, 40 wt.% $LaPO_4$, pure $LaPO_4$). X-ray diffraction analysis showed that only Al_2O_3 and $LaPO_4$ phases exist in the $Al_2O_3/LaPO_4$ composites with different $LaPO_4$ content even sintered up to 1600 °C. Bulk density, hardness and microstructures of the $Al_2O_3/LaPO_4$ composites are largely dependent on the $LaPO_4$ content and sintering temperature. Due to the layered structure of $LaPO_4$ and the weak interface between the Al_2O_3 and $LaPO_4$ phase, the 40 wt.% $Al_2O_3/LaPO_4$ composite can be easily machined using cemented carbide drills instead of conventionally diamond tools.

Keywords: B. Microstructure; C. Hardness; D. Al_2O_3

1. Introduction

Machining is emerging as an inevitable requirement for flexible use of advanced ceramics, especially for structural ceramics. However, the extremely high hardness of ceramics makes conventional machining very difficult or even impossible. In the past years, much research has been focused on the improvement of ceramic machinability [1–4]. Generally, two methods were used for improving the machinability of ceramic materials. One method is to introduce a weak interface phase or layer structured material in the matrix to facilitate crack deflection during machining. The materials are called compound machinable ceramics, such as mica-containing glass-ceramic [5]. The other method is the structure-design method, where the machinability of ceramics is optimized by adjusting the distribution of phase, porosity and three-dimensional macrostructure and microstructure, such as porous ceramics, graded machinable ceramics [6] et al.

$LaPO_4$ (lanthanum phosphate, monazite-type) is a suitable and effective oxide interface material, which exhibits high stability at high temperature in both reducing and oxidizing environment and shows good chemical compatibility with Al_2O_3. The $Al_2O_3/LaPO_4$ interface is weak enough to prevent crack growth by interfacial debonding and crack deflection. Therefore, $LaPO_4$ is commonly used as coating on alumina fibers in ceramic matrix composites (CMCs) [7].

Recently, according to the research of Davis and Marshall [8], two-phase composites consisting of $LaPO_4$ or $CePO_4$ with alumina, mullite, or zirconia could be cut and drilled using conventional tungsten carbide metal-working tools. $LaPO_4$ in the Al_2O_3 composites is quite stable and no reaction occurs between the two phases up to 1650 °C, provided the La:P ratio in the monazite is close to 1. The enhancement of machinability is attributed to a weak interface ($Al_2O_3/LaPO_4$ grain boundaries) and layered $LaPO_4$ phase in this composite. However, a systematic study on sintering behavior and microstructures of the $Al_2O_3/LaPO_4$ composites has not been reported.

In this paper, we discuss the microstructural evolution of $Al_2O_3/LaPO_4$ composites with different $LaPO_4$ additions, which were sintered at different temperatures. At

* Corresponding author. Tel.: +86+10-6277-2859; fax: +86+10-6277-1160.

E-mail address: rgwang99@mails.tsinghua.edu.cn (R. Wang).

0272-8842/02/$22.00
PII: S0272-8842(02)00083-4

the same time, we also investigated systematically the relationship between microstructure and hardness of the $Al_2O_3/LaPO_4$ composites with different $LaPO_4$ contents and sintering temperatures.

2. Experimental procedure

2.1. Powder preparation and sintering

As a major raw material, Al_2O_3 having a minimum α-phase content of 95 mass% were used. The median particle and crystal size of the aluminas ranged from 0.5 to 2 μm, their specific surface ranged from 8–11 to 1.5 m^2/g. The $LaPO_4$ powders were synthesized by mixing phosphoric acid with lanthanum oxide in a water bath. Lanthanum oxide was dissolved in diluted phosphoric acid with La to P of 1:1 in order to achieve $LaPO_4$ as a final product. The direct reaction between lanthanum oxide and phosphoric acid is a clean reaction with no by-products other than water according to the reaction

$$La_2O_3 + 2H_3PO_4 \rightarrow 2LaPO_4 + 3H_2O \quad (1)$$

In this process, La_2O_3 powders were slowly added to 85% H_3PO_4 (diluted by distilled water), large precipitates were formed immediately at the reaction site. Subsequently, these synthesized powders were washed several times with de-ionized water until the pH value of the filtered water became close to 7. All the chemicals used were of analytical reagent grade.

The $Al_2O_3/LaPO_4$ composite powders with different $LaPO_4$ contents were ball milled under ethyl alcohol with agate balls for 24 h and then dried using a rotary vaporizer. The resulting powders were uniaxially dry-pressed with 150 MPa in a cylindrical mold ($\phi 20\times6$ mm^2) to obtain the green compacts. The samples ($M_{Al_2O_3}$:M_{LaPO_4}=6:1, which ratio was chosen from literature [8] and considering the machinability of the composites) were sintered in a furnace (Nabertherm, Germany) at 1300, 1400, 1500 and 1600 °C respectively for 2 h in order to determine a suitable sintering temperature for the $Al_2O_3/LaPO_4$ composites, and then cooled down slowly to room temperature. The Al_2O_3/$LaPO_4$ composite powders with different $LaPO_4$ contents (pure Al_2O_3, 10 wt.% $LaPO_4$, 20 wt.% $LaPO_4$, 30 wt.% $LaPO_4$, 40 wt.% $LaPO_4$, pure $LaPO_4$) were sintered at 1600 °C for 2 h to investigate the relationship between $LaPO_4$ content and hardness, machinability and microstructures of the composites.

2.2. Characterization of microstructure and mechanical properties

The densities of the composites were measured by the Archimedes method. Theoretical density was calculated using the rule of mixture ($\rho=\rho_{LaPO_4}V_{LaPO_4}+\rho_{Al_2O_3}V_{Al_2O_3}$; $\rho_{LaPO_4}=5.07$ g/cm^3; $\rho_{Al_2O_3}=3.99$ g/cm^3). Scanning electron microscopy (Model Hitachi SEM-450, Japan and Model SEM LEO 1530, Germany) was used for the investigation of the microstructure. Ceramic crystalline phases were determined by X-ray diffraction (Model Automated D/Max-rb, Japan). Vickers's hardness (H_V) was determined on polished surfaces by using a load of 5 kg for 10 s. Eight indents were made at each specimen.

The machinability of the specimen was tested by using cemented carbide drills at 2500 rpm. A drop of water was placed at the drill tip at the beginning of each run.

3. Results and discussion

3.1. Chemical compatibility and densification

The chemical stability of $LaPO_4$ and Al_2O_3 in the $Al_2O_3/LaPO_4$ composites sintered at different temperatures for 2 h was investigated by analyzing the possible existing phases using X-ray diffraction (XRD). Figs. 1 and 2 show the corresponding XRD results. It can be seen that there are only Al_2O_3 and $LaPO_4$ phases in the composites with different $LaPO_4$ contents sintered up to 1600 °C. Apparently, no reaction occurred under this experiment condition. Therefore, it can be presumed that a weak interface was formed at the boundaries of Al_2O_3 and $LaPO_4$ grains (Figs. 4 and 8). This agrees with the results of D.B. Marshall [9].

The curve of bulk density vs sintering temperature for the composites containing the same content of $LaPO_4$ ($M_{Al_2O_3}$:M_{LaPO_4}=6:1, which ratio is chosen from literature [8] and considering the machinability of the composites) is shown in Fig. 3. The densities of the

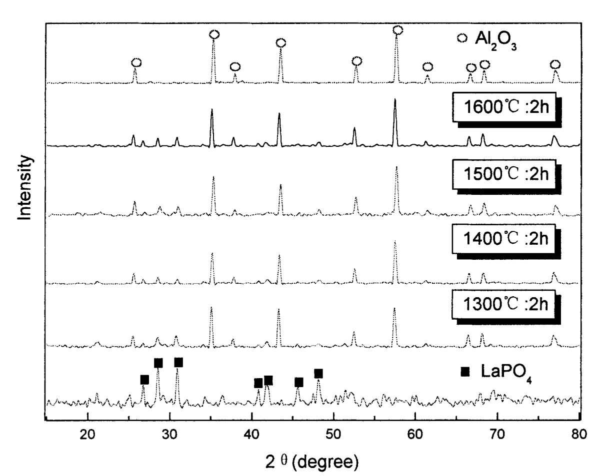

Fig. 1. XRD patterns of the $Al_2O_3/LaPO_4$ composites showing chemical compatibility at different sintering temperatures.

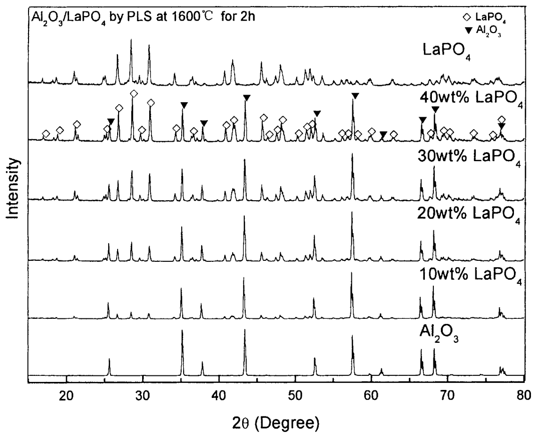

Fig. 2. XRD patterns of the $Al_2O_3/LaPO_4$ composites with different $LaPO_4$ contents.

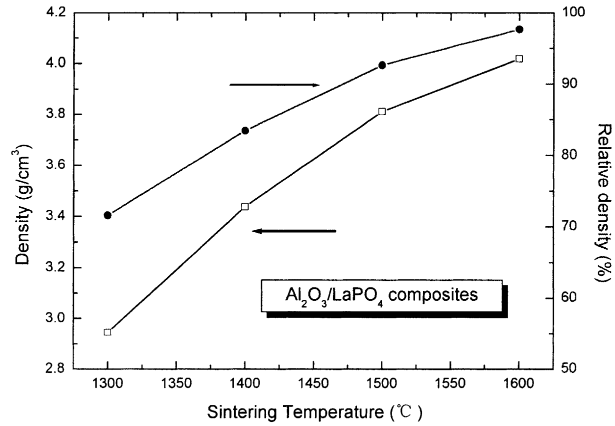

Fig. 3. Effect of sintering temperature on the bulk density and relative density of the $Al_2O_3/LaPO_4$ composites.

composites increase with increasing sintering temperature. When the sintering temperature reached 1600 °C, the relative density of the composite is close to theoretical density. Therefore, the investigation on the influence of the $LaPO_4$ content on the hardness, microstructure and densification of the composites chose 1600 °C as sintering temperature. Fig. 4 shows the microstructural evolution of the $Al_2O_3/LaPO_4$ composites sintered at different temperatures (1300, 1400, 1500 and 1600 °C) for 2 h. It can be seen that the densification improves with increased sintering temperature.

At a constant sintering temperature (1600 °C), the densities of the composites increased with the increasing $LaPO_4$ addition due to the high density of $LaPO_4$ ($\rho_{LaPO_4} = 5.07$ g/cm^3, where the theoretical density is determined using the lattice constants $a = 0.6837$, $b = 0.7077$ and $c = 0.6510$ nm). However, pure $LaPO_4$ ceramic obtains the maximal densification of the composites, and pure Al_2O_3 also has higher relative density than that of the $Al_2O_3/LaPO_4$ composites as shown in Table 1. That indicated the addition of $LaPO_4$ reduced the densification of the $Al_2O_3/LaPO_4$ composites. According to the microstructural observation, the reduction of relative density could be attributed to the creation of defects.

3.2. Hardness

Hardness is an important parameter as an indication of ceramic machinability. Generally, lower hardness, more excellent machinability. Vickers's hardness was measured on the polished surface of the composites. The variation of the average Vickers's hardness of samples ($M_{Al_2O_3}$:M_{LaPO_4} = 6:1) sintered at various temperatures is shown in Fig. 5. It can be noted that the lowest hardness value of 1.38±0.2 GPa was measured for the sample sintered at 1300 °C, whereas the maximum hardness value of 6.2±0.12 GPa was obtained for the sample sintered at 1600 °C. The general trend which can be observed in Fig. 5 is that the hardness increases with increased sintering temperature from 1300 to 1600 °C. The relatively low hardness obtained for samples sintered at low temperature was mainly attributed to the low densification of the material.

As is known, for the materials of having a similar densification, the hardness is governed by grain size. In general, high hardness values are found for fine-grained materials. In several fine grained/nanophase ceramics, an increase of Vickers's hardness (H_V) with decreasing grain size (d) according to the Hall–Petch relationship ($H_V = H_0 + \text{constant}/d^{-0.5}$) has been observed. In

Table 1
Sintered densities of the $Al_2O_3/LaPO_4$ composites by pressureless sintering at 1600 °C

Content of $LaPO_4$	Bulk density (g/cm^3)	Theoretical density (g/cm^3)	Relative density (% Th[a])
0	3.83	3.99	96.7
10	3.815	4.077	93.6
20	3.922	4.168	94.1
30	3.98	4.262	93.4
40	4.11	4.362	94.2
100	4.94	5.07	97.4

[a] Theoretical density: Al_2O_3 (3.99 g/cm^3); $LaPO_4$ (5.07 g/cm^3).

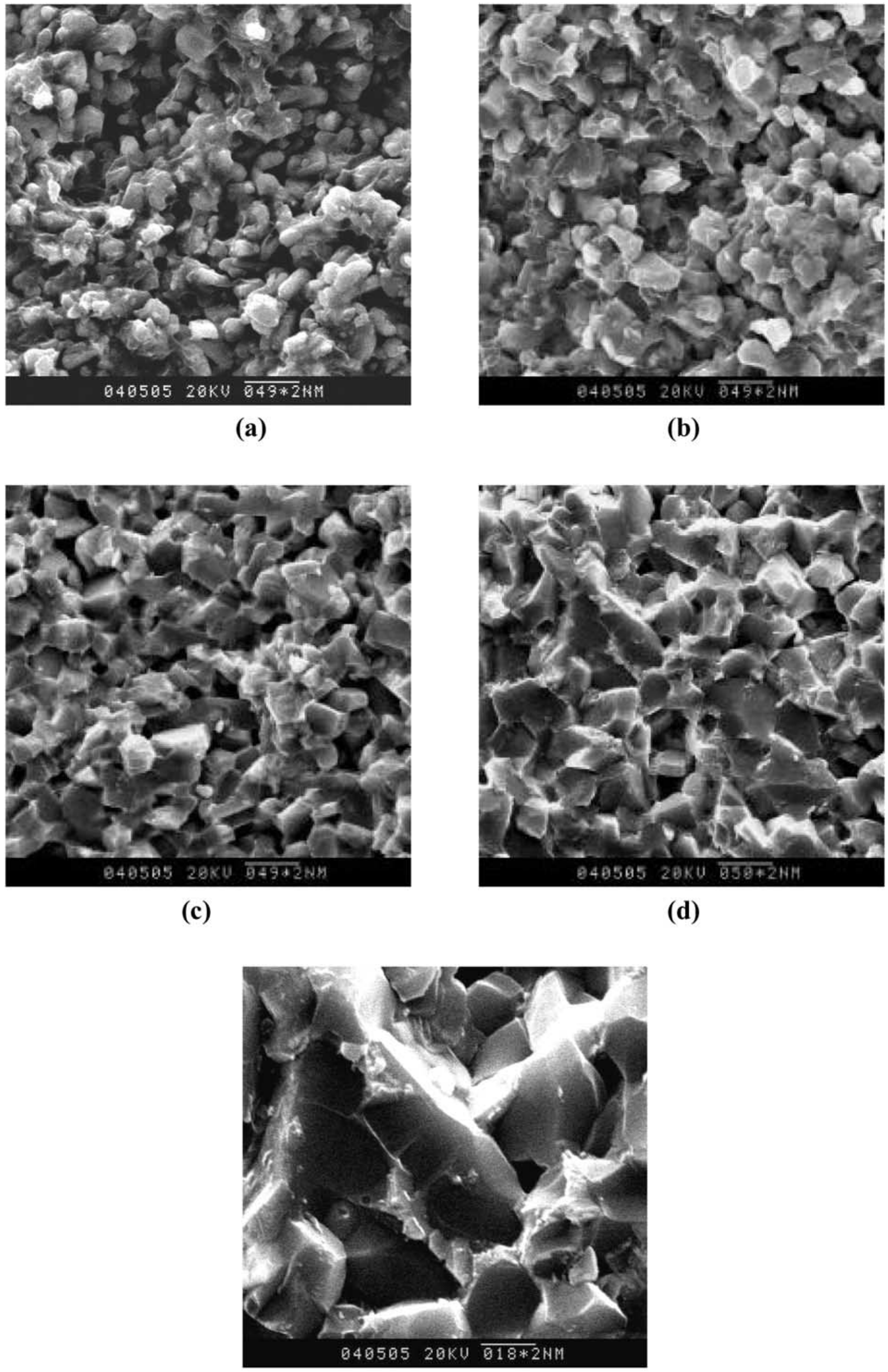

Fig. 4. SEM micrographs of $Al_2O_3/LaPO_4$ fracture surfaces at different sintering temperatures. (a) 1300 °C; (b) 1400 °C; (c) 1500 °C; (d) 1600 °C; (e) 1600 °C [magnified from (d)].

contrast, in this result (from Fig. 7, more $LaPO_4$ addition, smaller grain size of Al_2O_3), the grain size is not the controlling parameter for the hardness of the composites but rather the formation of weak interface between Al_2O_3 and $LaPO_4$ phases. Namely, more addition of $LaPO_4$ phase resulted in finer grain size and lower hardness of the composite.

Fig. 6 shows the relationship between the Vickers's hardness of the $Al_2O_3/LaPO_4$ composites and the $LaPO_4$ content. With the increased $LaPO_4$ addition, a steep decrease in the hardness of the $Al_2O_3/LaPO_4$ composites was observed. Because of the similar relative density of the sintered materials, the presence of the weak grain boundary phase resulted in a significant

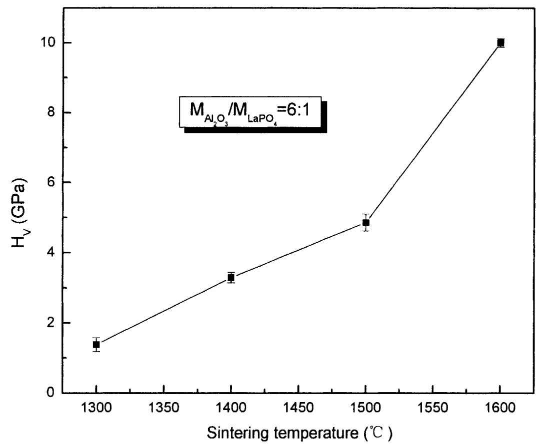

Fig. 5. Vickers's hardness vs sintering temperature of the Al_2O_3/ $LaPO_4$ composite.

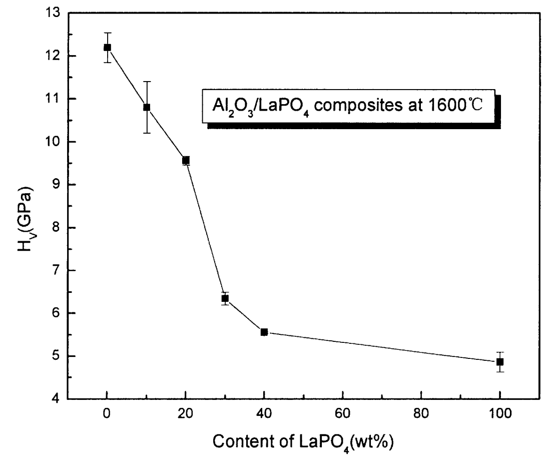

Fig. 6. Effect of $LaPO_4$ content on the Vickers's hardness of the $Al_2O_3/LaPO_4$ composites.

reduction in the hardness. Grain boundary sliding (migration) and easily delaminating of layered $LaPO_4$ phase will attribute to the decreased hardness value of the $Al_2O_3/LaPO_4$ composites with the increased $LaPO_4$ content. This reduced hardness leads to good machinability. When the $LaPO_4$ content increases up to 40 wt.%, the Vickers's hardness is reduced to 5.55 GPa. This value is close to that of machinable mica glass-ceramic [5] (3 GPa) and layered ternary compound Ti_3SiC_2 [10] (4–5 GPa).

3.3. Microstructure

The change in the hardness and machinability of the $Al_2O_3/LaPO_4$ composites is related closely to their microstructures. Fig. 4 shows the microstructural development of the $Al_2O_3/LaPO_4$ composites at various sintering temperatures. Cracks prefer to propagate along interfaces or are deflected into the $LaPO_4$ phase. There are many lateral cracks propagating along interfaces, but no crack is propagating perpendicularly through the Al_2O_3. This may be the main reason that the addition of $LaPO_4$ can improve the machinability of the $Al_2O_3/LaPO_4$ ceramic composites.

The addition of $LaPO_4$ serves two purposes: (i) it forms a fine, highly stable $LaPO_4$ phase, which pins the boundaries of Al_2O_3 and refines the grain size of Al_2O_3, and (ii) it segregates at the Al_2O_3 grain boundaries (Figs. 4e, 7e and f) and does not react with Al_2O_3 even at high temperature (1600 °C/2 h). This enhances the machinability of the composites by crack deflection along the weak interface between $LaPO_4$ and Al_2O_3 and along layer plane of $LaPO_4$ phase during cutting, grinding and drilling.

According to the study of Linan An [11], weak grain/ interface boundaries can promote the formation of bridging sites and residual thermal stresses, enhance the bridging intensity. Thus, ceramic materials can be toughened by grain bridging in the wake of propagating cracks. It has been demonstrated that the bridging effect can be enhanced by deliberately introducing microstructural heterogeneities. In the present study, $LaPO_4$ phase can play a similar role in the $Al_2O_3/LaPO_4$ composites.

The microstructural evolution of the $Al_2O_3/LaPO_4$ composites with different $LaPO_4$ contents is shown in Fig. 7. The pure Al_2O_3 has abnormal grain growth, and the transgranular fracture is the main fracture mode of alumina. $LaPO_4$ grains possess a layered crystal structure (Fig. 7d). Since layered $LaPO_4$ can be readily delaminated due to its low cleavage energy, fractures propagate parallel to the layer crystals. Crack deflections, branching and blunting during machining of layered crystal $LaPO_4$ help to prevent macroscopic fractures from propagation beyond the local cutting area. For the $Al_2O_3/LaPO_4$ composites, the layered structure $LaPO_4$ surrounding the Al_2O_3 grains is the main feature in the microstructure of this composite. At the same time, the increase of the $LaPO_4$ content inhibited the growth of Al_2O_3 grains. Fig. 7e and f shows the microstructures of 40 wt.% Al_2O_3/ $LaPO_4$ composite by second electron image and backscattered electron image. Most of the fracture mode belongs to intergranular fracture. This confirmed the formation of weak $Al_2O_3/LaPO_4$ interfaces and is the main reason of the improved machinability of this composite.

3.4. Machinability

The machinability of the 40 wt.% $Al_2O_3/LaPO_4$ composites using cemented carbide drills was investigated. Generally, diamond tools are used for the machining of advanced ceramics. Fig. 8 shows a hole made by cemented carbide drills on the 40 wt.% Al_2O_3/ $LaPO_4$ specimen. It can be seen that the $Al_2O_3/LaPO_4$ composite is successfully machined. However, due to the high hardness, the pure Al_2O_3 cannot be machined

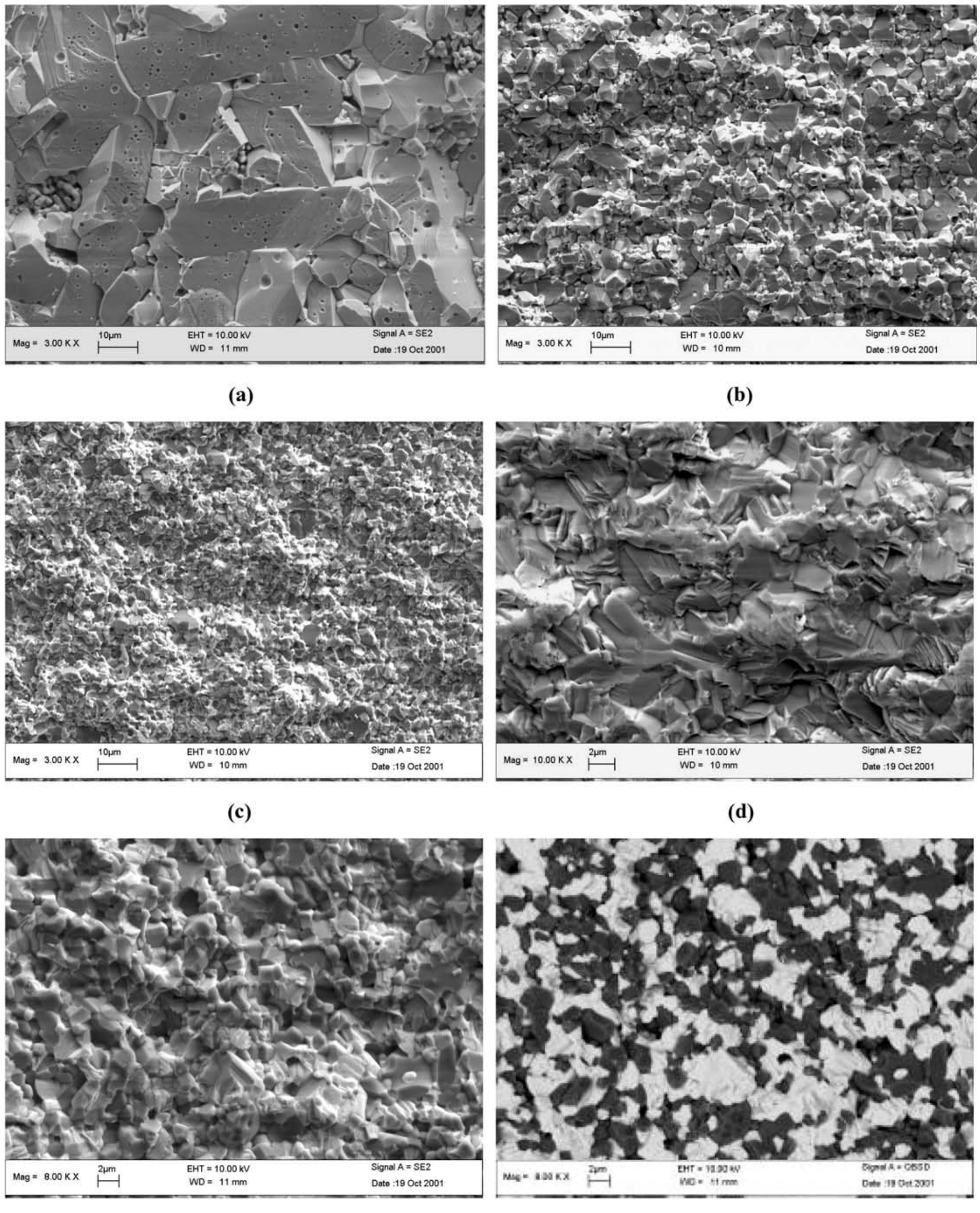

Fig. 7. SEM micrographs of $Al_2O_3/LaPO_4$ fracture surfaces with different $LaPO_4$ contents: (a) Al_2O_3; (b) 10 wt.% $LaPO_4$; (c) 30 wt.% $LaPO_4$; (d) $LaPO_4$; (e) 40 wt.% $LaPO_4$ (second electron image); (f) 40 wt.% $LaPO_4$ (backscattered electron image).

using such drills. As stated above, the layered structure $LaPO_4$ and the weak interface at the $Al_2O_3/LaPO_4$ grain boundaries are the main reason for the improvement of the machinability. Both of them enhance the crack deflection and avoid the catastrophic failure of the material during drilling. Other important factors including the wear of the tool, the cutting force vs drilling rate, the surface roughness of the work piece, the diffusion mechanism between the tool and the work piece, will be studied systematically in the future.

4. Conclusions

A dense and machinable $Al_2O_3/LaPO_4$ composite was successfully fabricated by adjusting the experimental conditions (sintering temperature and $LaPO_4$ content). XRD analysis indicated that there is good chemical compatibility between Al_2O_3 and $LaPO_4$ phase, no reaction occurred even at sintering temperatures up to 1600 °C. The segregation of $LaPO_4$ at the Al_2O_3 grain boundaries enhances the crack deflection and avoid the

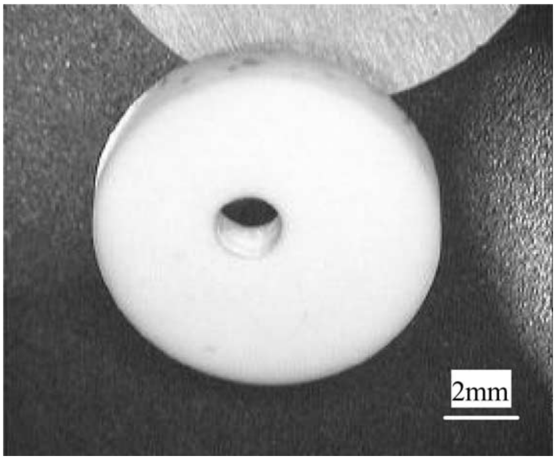

Fig. 8. Machinable $Al_2O_3/LaPO_4$ ceramic composite using cemented carbide drill.

catastrophic destruction of the sample during drilling. Due to the weakness of the $LaPO_4$ phase and the weak boundaries between $LaPO_4$ and Al_2O_3, the machinability of the composite can be improved remarkably. The 40 wt.% $Al_2O_3/LaPO_4$ specimen can be easily machined using cemented carbide drills instead of conventional diamond tools.

References

[1] D.G. Grossman, Machinable glass-ceramics based on tetrasilicic mica, J. Am. Ceram. Soc. 55 (9) (1972) 446–449.

[2] M.W. Barsoum, T. El-Raghy, Synthesis and characterization of a remarkable ceramic: Ti_3SiC_2, J. Am. Ceram. Soc. 79 (7) (1996) 1953–1956.

[3] N.P. Padture, C.J. Evans, H.H.K. Xu, et al., Enhanced machinability of silicon carbide via microstructural design, J. Am. Ceram. Soc. 78 (1) (1995) 215–217.

[4] AkiraYamakawa Chihiro Kawai, Machinability of high-strength porous silicon nitride ceramic, J. Ceram. Soc. Jap. 106 (11) (1998) 1135–1137.

[5] H.K. Xu Hockin, J. Said, Scratching and grinding of a machinable glass-ceramic with weak interfaces and rising T-curve, J. Am. Ceram. Soc. 78 (2) (1995) 497–500.

[6] W. Pan, R.G. Wang, Machinable ceramics and its graded design, Rare Metal Mater. Eng. 29 (Suppl.) (2000) 84–88.

[7] T.J. Hwang, M.R. Hendrick, Combustion chemical vapor deposition (CCVD) of $LaPO_4$ monazite and beta-alumina on alumina fibers for ceramic matrix composites, Mater. Sci. Eng. A 244 (1) (1998) 91–96.

[8] J.B. Davis, D.B. Marshall, Machinable ceramics containing rare-earth phosphates, J. Am. Ceram. Soc. 81 (8) (1998) 2169–2175.

[9] D.B. Marshall, P.E.D. Morgan, High-temperature stability of the Al_2O_3-$LaPO_4$ system, J. Am. Ceram. Soc. 81 (4) (1998) 951–956.

[10] M.W. Barsoum, Layered machinable ceramics for high temperature applications, Scripta Mater. 36 (5) (1997) 535–541.

[11] An Linan, Indentation fatigue in random and textured alumina composites, J. Am. Ceram. Soc. 82 (1) (1999) 78–82.